Amyloid fibrils: modulation of formation and structure by copper(II)

Vincent Pradines, Alina Jurca Stroia and Peter Faller*

Received (in Montpellier, France) 19th December 2007, Accepted 23rd January 2008
First published as an Advance Article on the web 19th February 2008
DOI: 10.1039/b719556g

The role of Cu^{II}-complexation of amyloidogenic peptides on the formation and structure of aggregates were analyzed in order to obtain a general insight into modulation of peptide aggregation by metal ions. The results mimicked various facets of biological relevant peptides/protein-aggregation. Important mechanistic features are the ability of Cu^{II} to associate the peptides by bridging coordination, the structural changes induced by Cu^{II} binding and their effect on peptide–peptide interactions.

Introduction

Interest in the structure and formation of amyloid fibrils originates from their association with several, often neurodegenerative diseases. Although peptides or proteins alone are able to form fibrils *in vitro*, other factors, such as metal ions, have been proposed to play an important role by modulating the formation of amyloid fibrils. Cu^{II} has been shown to be able to bind to several amyloid-forming peptides/proteins and modulating their aggregation behaviour.[1] Depending on the peptide/protein and the conditions, Cu^{II} showed inhibiting or accelerating effects on fibril formation.[2–8] Cu^{II} affected also the structure of the amyloid aggregates, as in certain cases Cu^{II} was promoting amorphous aggregates rather than amyloid fibrils.[9]

In order to get a general insight into molecular basis for this modulating effect of Cu^{II} on the aggregation of peptides/proteins, we used short peptides as models. Their preparation and handling is relatively easy, but can provide important insight on basic mechanisms.[10] Three peptides were selected, originating from the amyloid-β peptide (Aβ), which is one of the best studied and interaction with Cu^{II} has been shown to be relevant.[11–13] The three peptides consist of their amino acid sequence 14–23, 11–23 and 11–28 of full length Aβ (Fig. 1).

Peptide Aβ14-23 was chosen because it has been shown to be one of the shortest fragments of Aβ able to form fibrillar structures, which showed the typical interaction with thioflavin T (ThT).[14] Moreover, this peptide still contains one His known to ligate Cu^{II}.[11,15–17] Peptide Aβ11-23 has an N-terminal extension of three amino acids of the type H_2N–Xxx-Xxx-His. This motif, called ATCUN, is known to bind Cu^{II}.[18] Aβ11-23 contains also the His dyad implicated in Cu^{II}-binding of the full-length Aβ.[12] However, this peptide has so far not been studied in term of aggregation properties. In contrast the Aβ11-28, containing the same N-terminal extension, is known to form amyloid fibrils (without Cu^{II}).[19] Under non-aggregating condition Aβ11-28 was shown to bind Cu^{II} in the ATCUN motif (Fig. 2).[20]

Laboratoire de Chimie de Coordination du CNRS, Université Paul Sabatier, 205 route de Narbonne 31077, Toulouse, France. E-mail: faller@lcc-toulouse.fr; Fax: +33 5 61 55 30 03; Tel: +33 5 61 33 31 62

In the present study, the aggregation kinetic and fibril structures of the model-peptides Aβ14-23, Aβ11-23 and Aβ11-28 were compared in the presence and absence of Cu^{II} (Fig. 3).

Results and discussion

The aggregation kinetics was directly followed by turbimetry and ThT fluorescence (ThT is a dye known to interact specifically with amyloid type fibrils).[21] The turbidity measurements were confirmed at several time points by measuring the peptide concentration in the supernatant after centrifugation (not shown). Aβ14-23 in the absence of Cu^{II} exhibits a fast formation of amyloid-type aggregates (Fig. 3(a)). The addition of Cu^{II} showed a dramatic effect and turbidity measurements suggest an accelerated and more intense aggregation. This was confirmed by transmission electron microscopy (TEM) showing more fibrils in the presence of Cu^{II} (Fig. 3(b)). The morphology did not change significantly of the amyloid type fibrils upon addition of Cu^{II}. The ThT fluorescence of Cu^{II}–Aβ14-23 was very low, which seemed to be in contradiction with the large amount of fibrils seen in the TEM. This can be explained by the fluorescence quenching of ThT by the paramagnetic Cu^{II}, because UV-Vis absorption spectroscopy clearly showed the binding of ThT to Cu^{II}–Aβ14-23. The ThT-binding to fibrils is accompanied by a red shift of the band at 408 nm,[21] which was at least as marked for Cu^{II}–Aβ14-23 than for Aβ14-23 (Fig. 4).

In contrast, the second peptide Aβ11-23 in the presence and absence of Cu^{II} showed only few aggregates by TEM, and remarkably with a different structure: amorphous for Aβ11-23 and fibrillar for Cu^{II}–Aβ11-23. Turbidity and ThT fluorescence did not change over a period of 10 h. In order to confirm the significance of the aggregates detected by TEM, the concentration of Aβ11-23 (and Cu^{II}) was increased. Indeed, the turbidity increased and TEM showed more aggregates, predominantly amorphous for Aβ11-23 and fibrillar for

Aβ11-28: NH_3^+-EVHHQKLVFFAEDVGSNK-COO^-
Aβ11-23: NH_3^+-EVHHQKLVFFAED-COO^-
Aβ14-23: NH_3^+-HQKLVFFAED-COO^-

Fig. 1 Sequence of Aβ11-28, 11–23 and 14–23.

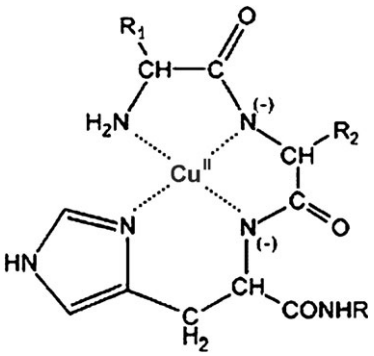

Fig. 2 ATCUN motif: Cu^{II} bound to N-terminal Xxx-Xxx-His-... (Xxx represents amino acid).

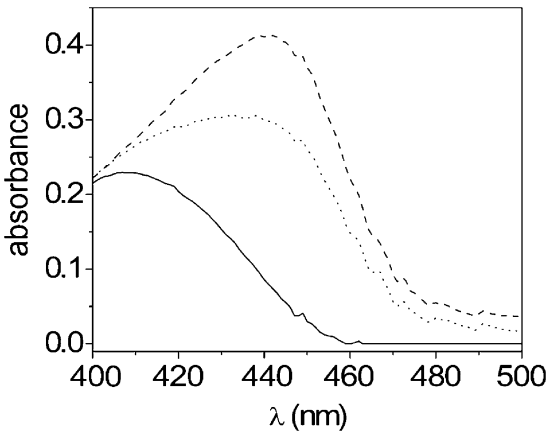

Fig. 4 UV-Vis absorption spectra of the ThT (10 μM): (—) ThT alone in solution (Hepes buffer, 20 mM, pH 7, 4); (···) in the presence of aggregated Aβ14-23; (--): in the presence of aggregated Aβ14-23 and Cu^{II}.

Cu^{II}-Aβ11-23 (Fig. 7(a) and (c)). After longer incubation of amorphous Aβ11-23 without Cu, fibrils were also observed (Fig. 7(b)).

The third peptide Aβ11-28 aggregated into fibrils (Fig. 3(c)) as already reported in the literature.[19] Upon addition of Cu^{II} to Aβ11-28 only very few fibrils were formed. Interestingly, these structures were significantly different from the fibrils in the absence of Cu^{II}. They were generally larger and had a rougher surface. In agreement, ThT fluorescence and turbidity increased modestly (Fig. 3(d)).

Taken together, these results showed that Cu^{II} can have dramatic effects on the formation and structure of amyloid fibrils. Cu^{II} accelerates and increases fibril formation of Aβ14-23, but reduces the fibril formation of Aβ11-28, or decelerates aggregation but pushes the peptide to form fibrils rather than amorphous aggregates (Aβ11-23). Thus the three peptides reflect several features of Cu-modulated aggregation of amyloid peptides and can be considered as valuable models.

In order to get an insight into the underlying mechanism of these different effects of Cu, several structural studies were undertaken. The peptides Aβ11-28 and Aβ11-23 contain the N-terminal sequence of the type Xxx-Xxx-His (ATCUN), but also the His-His dyad, both reported to be able to bind Cu^{II}. EPR and absorption spectroscopy revealed the typical features of Cu^{II} in the ATCUN motif for soluble Cu^{II}–Aβ11-28[20] and Cu^{II}–Aβ11-23. The absorption spectrum of Cu^{II}–Aβ11-28 shows a band a 520 nm with ε of about 100 cm^{-1} M^{-1}. This is typical for the d–d bands of Cu in the ATCUN motif. Titration of Cu^{II} to Aβ11-28 suggested strongly that 1 equivalent Cu binds to Aβ11-28 in the ATCUN motif (Fig. 5, inset). EPR of Cu^{II}–Aβ11-28 showed a spectrum with $g_{\|}$ of 2.18, $g_{\perp}$ of 2.05 and a $a_{\|}$ of 205 G, in line with the ATCUN motif (Fig. 6). Moreover, the superhyperfine couplings with the nitrogens can be observed. Although the expected nine lines originated from the coupling with the four nitrogens can not be unambiguously identified, the overall spectrum suggests strongly the binding of Cu in the ATCUN motif. Cu^{II}–Aβ11-

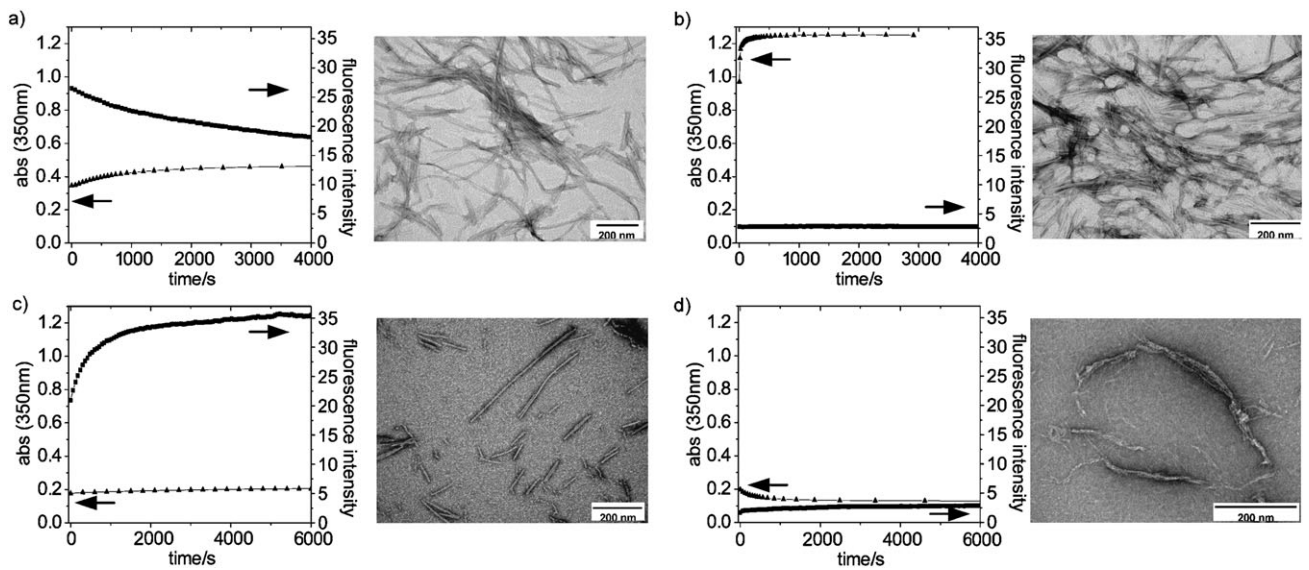

Fig. 3 Negatively stained TEM images and aggregation kinetics followed by turbimetry (UV-Vis, λ = 350 nm, left scale) and fluorescence ([ThT] = 100 μM, λ_{ex} = 437 nm, λ_{em} = 485 nm, right scale) in 20 mM Hepes pH = 7.4, [Aβ-peptide] = 300 μM: (a) Aβ14-23; (b) Cu^{II}–Aβ14-23, [Cu^{II}] = 270 μM; (c) Aβ11-28; (d) Cu^{II}–Aβ11-28, [Cu^{II}] = 270 μM.

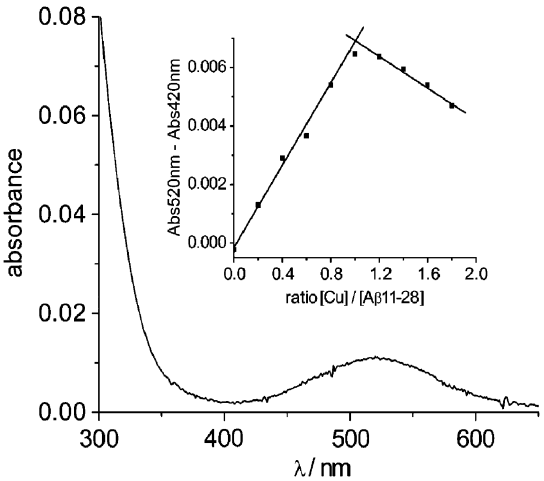

Fig. 5 UV-Vis spectrum of Cu^{II}–Aβ11-28 showing the d–d band at 520 nm for 1 : 1 stoichiometry; inset: titration of Aβ11-28 (100 μM) by Cu^{II}.

23 showed almost identical absorbance and EPR parameters (not shown). The studies were extended in order to see if these complexes were monomeric and if coordination changes with time and hence with generation of aggregates. Mass spectrometry and size-exclusion chromatography showed that Cu^{II}–Aβ11-23 and Cu^{II}–Aβ11-28 formed monomeric and stoichiometric complexes prior to aggregation (not shown). Mass spectrometric analysis of fragmentation of Cu^{II}–Aβ11-28 and Cu^{II}–Aβ11-23 confirmed the binding of the Cu^{II}–ATCUN motif. The most intense peak upon fragmentation had a mass of 429.4 Da, which corresponds to the isolated ATCUN motif plus CO, *i.e.* Cu^{II}–EVH–C═O. Furthermore, time dependence measurements of absorption and EPR did not show any significant changes, indicating that the Cu-coordination environment of Aβ11-28 did not change upon aggregation. Taken together, in the case of Aβ11-23 and Aβ11-28, Cu is bound as a monomeric complex in an ATCUN motif in the soluble and aggregated state.

His structural insights help to rationalize the observation that Cu^{II}-binding does inhibit but not suppress the aggregation and fibril formation of Aβ11-28. In the absence of Cu^{II}, Aβ11-28 aggregates probably in antiparallel β-sheets as reported for similar Aβ model-peptides.[22] As Cu^{II} is bound in a

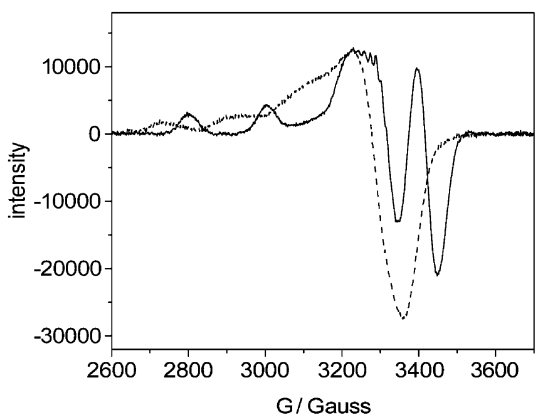

Fig. 6 EPR spectrum of Cu^{II}–Aβ11-28 (—) and Cu^{II}–Aβ14-23 (--).

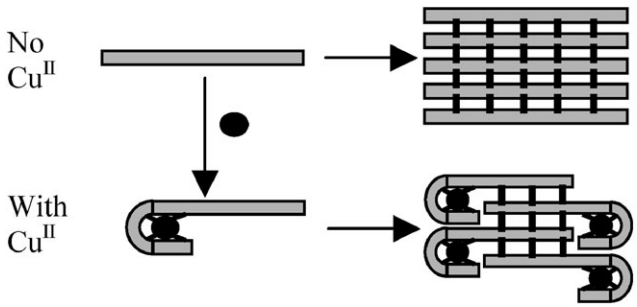

Scheme 1 Cartoon explaining the inhibition of Aβ11-28 fibril formation by Cu^{II}: Cu^{II} (black circles) binds to Aβ11-28 (grey rods) as a monomeric complex and reduces the number of H-bonds (black sticks) of the β-sheet in the fibrils compared to the fibrils without Cu^{II}.

monomeric complex and no indication of a change in coordination was found during aggregation, it can be proposed that aggregation has to occur *via* pure peptide–peptide interaction and not *via* bridging metal ions. Cu^{II}-binding to the N-terminal H_2N–Glu-Val-His in the ATCUN motif hampers the participation of these three amino acids in the β-sheet structure, since the amino acids are wrapped around the metal and not straight aligned as necessary to form the H-bonds in a beta-sheet. This would reduce the number of hydrogen bonds formed and hence destabilizes the fibrils (Scheme 1).

The peptide Aβ11-23 is the least hydrophobic and hence the least prone to aggregate. At concentration where Aβ14-23 and Aβ11-28 aggregate a lot, Aβ11-23 aggregates very little. At higher concentration (500 μM), Aβ11-23 forms amorphous (*i.e.* unordered) aggregates very rapidly and in high amounts (Fig. 7).

Formation of amorphous aggregates can be observed for almost all proteins at high concentrations.[23] Again the addition of Cu^{II} has a dramatic effect on kinetics and structure, as Aβ11-23 aggregates much more slowly and forms mostly fibrils (Fig. 7(c)). Cu^{II} binds to Aβ11-23 in the ATCUN motif as a monomeric complex. This results in the release of three protons and hence the net charge increases (from −2 to −3). The stronger repulsion could explain the slower aggregation rate, which may favour the formation of fibrils over amorphous aggregates.

In the case of Aβ14-23, Cu^{II}-binding enhanced the formation of amyloid-type fibrils. This peptide does not contain the monomeric ATCUN motif, and thus is likely to have ligands from more than one peptide. The EPR spectrum (Fig. 6) showed a major component with a $g_{\|}$ of 2.06, a $g_{\perp}$ of 2.26 and a $a_{\|}$ of 170 G, which fits best with an environment of three nitrogen and one oxygen,[24] the latter likely stemming from a carboxylate.[16] The EPR did not show time-dependence, but aggregation was too fast to trap the monomeric state. No coupling between the Cu^{II} centers was observed, indicating that the Cu^{II} sites in the fibrils are relatively distant (>4 Å) and a bridging His between two Cu^{II} can be excluded.[1] ^{1}H NMR studies of Aβ14-23 showed a drastic loss of intensity upon Cu^{II} complexation in line with aggregation. At substoichiometric addition of Cu^{II}, the resonances of His14 showed the highest enlargement, indicating that Cu^{II} binds to His14 (Fig. 8).

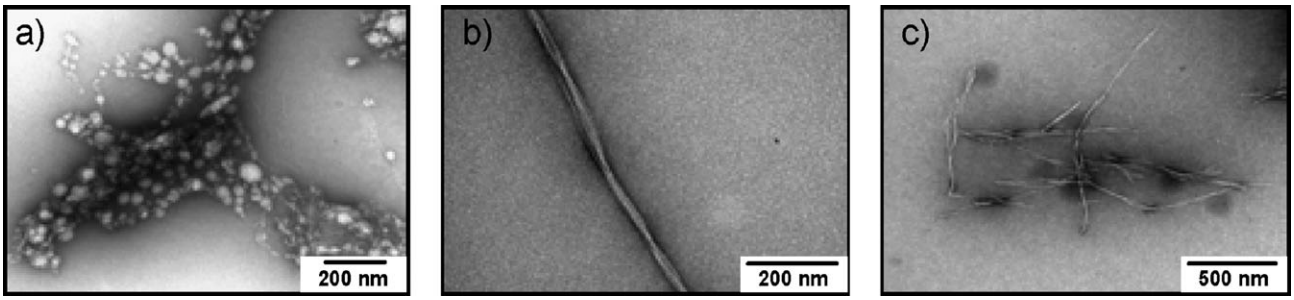

Fig. 7 TEM images of Aβ11-23 aggregates. In the absence of Cu^{II}: (a) after 2 h and (b) after 60 h, (c) with Cu^{II} after 60 h of incubation.

Cu-binding to a N-terminal His *via* the imidazole and amine is well established for peptide with a N-terminal His.[1] Taken together, the acceleration of Aβ14-23 fibril formation by Cu can be rationalized by postulating a bridging Cu, *i.e.* Cu binds in-between two (or more) Aβ14-23 and hence stabilizes the aggregation (Scheme 2).

It can be proposed that Cu^{II} binds to the N-terminal His as well as one of the C-terminal carboxylates, and thus linking the peptides together without disturbing the antiparallel beta-sheet arrangement. This would be in agreement with similar type of fibrils observed with and without Cu, as well as the spectroscopy suggesting Cu-binding to His and a carboxylate. Note that carboxylates are only present at the C-terminus (Glu22-Asp23–COO^-), *i.e.* opposite of the N-terminal His.

Thus taken together, it is proposed that the different binding mode of Cu, in particular the ability to bridge two peptide molecules (Scheme 2) or not (Scheme 1) can have an impact on structure and kinetics of aggregation.

These results give very general insight into the mechanisms of modulation of amyloid formation by Cu^{II}. It, however, does not give specific insights for the particular case of full length amyloid-beta, as the peptides used in the present study are truncated and do not contain the entire Cu-binding site.

In a very recent study, Dong *et al.*[25] reported results related to the present. They showed that Cu modulates the aggregation of the two peptides HHQALVFFA and Ac-HAQKLVFFA. In the former case Cu inhibits fibril formation and in the latter case Cu accelerated aggregation. The stoichiometry of Cu to peptide was 0.5 for both, and it was proposed that the Cu is coordinated by two different peptide molecules (*i.e.* bridging Cu). The promotion of Ac-HAQKLVFFA aggregation by Cu was attributed to a bridging Cu bound to two His along the hydrogen bonding direction. In contrast to that, in the present model the Cu promotes fibril formation with Aβ14-23 by a stoichiometric binding and by bridging between histidine and carboxylate and along the hydrogen binding direction but also perpendicular to it (Scheme 2).

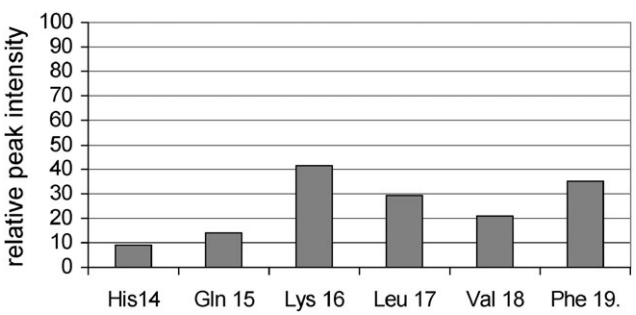

Fig. 8 ^{1}H NMR spectrum of Aβ14-23: relative peak intensity of Aβ14-23 with 0.5 equivalent of Cu compared to Aβ14-23.

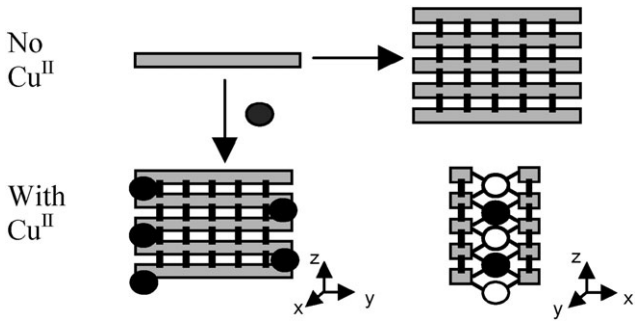

Scheme 2 Cartoon explaining the acceleration of the formation of Aβ14-23 fibrils by Cu^{II}. Cu^{II} (black circles) forms bridges between C- and N-termini of different Aβ14-23 (grey rods). As such it accelerates the fibril formation compared to the fibrils formed in the absence of Cu (black sticks symbolize the H-bonds in the β-sheets).

Concerning the inhibition of HHQALVFFA[25] and Aβ11-28 by Cu-binding, the mechanism seems to be different. It was suggested that Cu is able to bridge two molecules of HHQALVFFA, but does not stabilize the fibril formation. In contrast, for the peptide Aβ11-28 containing the ATCUN motif, Cu is clearly bound in a 1 : 1 complex and thus not able to bridge two molecules of Aβ11-28. Hence we assigned the inhibition of Aβ11-28 aggregation by Cu to the stabilization of the monomeric Aβ11-28, in a structure less prone to aggregation (Scheme 1).

The observation for Aβ11-23, that the Cu binding can alter the structure of the aggregation structure from amorphous to fibrils, has not been described for Aβ13-21 or one of their derivatives.

Conclusion

In conclusion, the Cu^{II} binding to the model peptides Aβ14-23, Aβ11-23, and Aβ11-28, revealed that Cu^{II} can modulate dramatically the formation and structure of amyloid aggregates. This can be directly related to their binding mode. An important feature for understanding the Cu^{II}–associate aggregation are the ability of Cu^{II} to associate the peptides by bridging coordination, the structural changes induced by Cu^{II} binding and their effect on peptide–peptide interactions.

Experimental

Aβ11-23/11-28/14-23 sample preparation

The peptides Aβ11-23 (sequence Glu-Val-His-His-Gln-Lys-Leu-Val-Phe-Phe-Ala-Glu-Asp), Aβ11-28 (sequence Glu-Val-His-His-Gln-Lys-Leu-Val-Phe-Phe-Ala-Glu-Asp-Val-Gly-Ser-Asn-Lys) and Aβ14-23 (sequence His-Gln-Lys-Leu-Val-Phe-Phe-Ala-Glu-Asp) were either purchased from EZBiolab (Westfield, IN, USA) and Genscript Corporation (Piscataway, NJ, USA). The stock solutions of peptides were prepared by dissolving the peptides in pure water (resistivity = 18 MΩ cm^{-1}), which resulted in a final pH was about 2. At that pH no significant aggregation occurred. The stock solutions were stored at 253 K. The peptide concentrations were determined by using the molar extinction coefficient $\varepsilon = 390\ M^{-1}\ cm^{-1}$ of the two phenylalanine at 258 nm.[26] (as phenylalanine does not absorb at 275 nm, the absorption at that wavelength was subtracted in order to remove contributions from the buffer or baseline shifts). Aggregation of peptides in the presence and absence of Cu^{II} were performed by dissolving peptides from a stock solution in a 20 mM Hepes buffer pH 7.4. Cu^{II} was generally added slightly substoichiometric (0.9 equivalent) to avoid unspecific effects of excess Cu^{II}. However, several control experiments with 1.0 equivalent Cu^{II} showed no significant difference.

Size exclusion chromatography

Analytical size exclusion chromatography of the peptides was performed at room temperature on a Superdex 75 10/300 GL column with an AKTA instrument (Amersham Pharmacia Biotech) under isocratic condition. Absorption was recorded at wavelengths of 220, 257 and 520 nm. The calibration of the column has been performed according to ref. 7. After equilibrating the column with elution buffer (20 mM Hepes, 100 mM NaCl, pH 7.4, flow rate: 0.8 mL min^{-1}), 100 μL peptides samples at 100 μM were injected.

Absorption spectroscopy (UV-Vis) and turbimetry

UV-visible absorption spectra were recorded at room temperature with a Agilent 8453 spectrometer connected to a personal computer (UV-Vis ChemStation, Rev.A.10.01 software), in a 1-cm path length quartz cuvette.

Turbidity measurements were done by measuring absorbance at 350 nm. Peptides concentrations were 300 μM in 20 mM Hepes pH 7.4.

NMR spectra

NMR spectra were collected using a Bruker Avance 500 spectrometer equipped with a 5-mm triple resonance inverse *Z*-gradient probe. All chemicals shifts for ^1H are relative to tetramethylsilane. ^1H NMR spectra were collected at 293 K in 90% H_2O–10% D_2O. Suppression of the water signal was achieved with a WATERGATE sequence. Spectra processing was performed using XWINNMR 3.5 software. The addition of Cu^{II} to Aβ11-23, Aβ14-23 and Aβ11-28 was carried out at 293 K. The peptide (0.5 mM) was dissolved in 0.5 ml, 50 mM tris(hydroxymethyl)aminomethane (Tris)-d_{11} buffer. Cu^{II} was added as chloride salts from a concentrated stock solution (10 mM) in order to keep the concentration of peptide almost constant (volume changes were below 5%). The pH was checked after each addition (and if necessary readjusted). In the case of the Aβ14-23, the well resolved peaks were used to monitor the effect of Cu^{II} on the peak intensity, *i.e.* the protons at position 4 of the imidazole ring for His, the β-protons of Gln15, the δ-protons of Lys16, the δ-protons of Leu17, the γ-protons of Val18 and the aromatic protons of Phe19 and Phe20.

EPR spectra

X-Band EPR data were recorded using an Elexsys ESP 500, operating at a microwave frequency of approximately 9.5 GHz. All spectra were recorded using a microwave power of 20 mW across a sweep width of 1500 G (centered at 3100 G) with a modulation amplitude of 10 G. Samples were frozen in quartz tube, with addition of 10% glycerol as a cryo-protectant in 20 mM Hepes. Experiments were carried out at 108 K using a liquid-nitrogen cryostat.

Fluorescence spectroscopy

Fluorescence spectra were collected in 96 well microplate by using a flx-Xenius spectrophotometer (SAFAS. S.A.) connected to a personal computer. Thioflavin T, peptides and if necessary Cu^{II} were mixed in Hepes buffer 20 mM pH 7.4. The time course of Thioflavin T fluorescence was measured (excitation 437 nm; emission 485 nm). The final concentration of peptides and thioflavin were 300 and 100 μM, respectively. Similar results were obtained at lower ThT concentrations (10 μM).

Electronic microscopy

5 μL of peptide samples were applied on EM grids, washed with 5 μL of milliQ water and negatively stained with an aqueous solution (5 μL) of uranyl acetate (1% w/w). Samples were air-dried and examined with JEOL 1011 transmission electronic microscope operating at an accelerating voltage of 100 kV.

Mass spectrometry

Mass spectrometry analyses were performed on a triple quadrupole API 365 (PE Sciex) equipped with an electrospray source. The acquisition system and the data processing for the set-up used Analyst 1.4 software (MS conditions: DP: 34 V, FP: 200 V, mass range: 600–2200; MS-MS conditions: collision energy (CE): 40 au). Peptides at 100 μM with and without 1 equivalent of Cu^{II} were prepared in a 20 mM ammonium acetate pH = 7 were directly injected (5 μL min^{-1}) in the mass spectrometer.

Acknowledgements

We thank Vincent Collière for the TEM images, Yannick Coppel for the NMR, Lionel Rechignat and Alain Mari for the EPR experiments, and Catherine Claparols and Nathalie Martin for the Mass Spectrometry measurements.

References

1. E. Gaggelli, H. Kozlowski, D. Valensin and G. Valensin, *Chem. Rev.*, 2006, **106**, 1995–2044.
2. C. S. Atwood, R. D. Moir, X. Huang, R. C. Scarpa, N. M. E. Bacarra, D. M. Romano, M. A. Hartshorn, R. E. Tanzi and A. I. Bush, *J. Biol. Chem.*, 1998, **273**, 12817–12826.
3. J. Zou, K. Kajita and N. Sugimoto, *Angew. Chem., Int. Ed.*, 2001, **40**, 2274–2277.
4. C. Exley, *J. Alzheimers Dis.*, 2006, **10**, 173–177.
5. A. Khan, A. E. Ashcroft, V. Higenell, O. V. Korchazhkina and C. Exley, *J. Inorg. Biochem.*, 2005, **99**, 1920–1927.
6. O. V. Bocharova, L. Breydo, V. V. Salnikov and I. V. Baskakov, *Biochemistry*, 2005, **44**, 6776–6787.
7. C. Talmard, L. Guilloreau, Y. Coppel, H. Mazarguil and P. Faller, *ChemBioChem*, 2007, **8**, 163–165.
8. L. E. Wilkinson-White and S. B. Easterbrook-Smith, *Biochemistry*, 2007, **46**, 9123–9132.
9. E. House, J. Collingwood, A. Khan, O. Korchazkina, G. Berthon and C. Exley, *J. Alzheimers Dis.*, 2004, **6**, 291–301.
10. J. Dong, J. E. Shokes, R. A. Scott and D. G. Lynn, *J. Am. Chem. Soc.*, 2006, **128**, 3540–3542.
11. D. G. Smith, R. Cappai and K. J. Barnham, *Biochim. Biophys. Acta, Biomembr.*, 2007, **1768**, 1976–1990.
12. P. A. Adlard and A. I. Bush, *J. Alzheimers Dis.*, 2006, **10**, 145–163.
13. L. Guilloreau, S. Combalbert, A. Sournia-Saquet, H. Mazarguil and P. Faller, *ChemBioChem*, 2007, **8**, 1317–1325.
14. L. O. Tjernberg, D. J. E. Callaway, A. Tjernberg, S. Hahne, C. Lilliehook, L. Terenius, J. Thyberg and C. Nordstedt, *J. Biol. Chem.*, 1999, **274**, 12619–12625.
15. C. D. Syme, R. C. Nadal, S. E. J. Rigby and J. H. Viles, *J. Biol. Chem.*, 2004, **279**, 18169–18177.
16. J. W. Karr, H. Akintoye, L. J. Kaupp and V. A. Szalai, *Biochemistry*, 2005, **44**, 5478–5487.
17. L. Guilloreau, L. Damian, Y. Coppel, H. Mazarguil, M. Winterhalter and P. Faller, *JBIC, J. Biol. Inorg. Chem.*, 2006, **11**, 1024–1038.
18. C. Harford and B. Sarkar, *Acc. Chem. Res.*, 1997, **30**, 123–130.
19. P. E. Fraser, J. T. Nguyen, W. K. Surewicz and D. A. Kirschner, *Biophys. J.*, 1991, **60**, 1190–1201.
20. T. Kowalik-Jankowska, M. Ruta-Dolejsz, K. Winiewska and L. Lankiewicz, *J. Inorg. Biochem.*, 2002, **92**, 1–10.
21. H. LeVine, *Methods Enzymol.*, 1999, **309**, 274–284.
22. A. T. Petkova, G. Buntkowsky, F. Dyda, R. D. Leapman, W.-M. Yau and R. Tycko, *J. Mol. Biol.*, 2004, **335**, 247–260.
23. F. Rousseau, J. Schymkowitz and L. Serrano, *Curr. Opin. Struct. Biol.*, 2006, **16**, 118–126.
24. J. Peisach and W. E. Blumberg, *Arch. Biochem. Biophys.*, 1974, **165**, 691–708.
25. J. Dong, J. M. Canfield, A. K. Mehta, J. E. Shokes, B. Tian, W. S. Childers, J. A. Simmons, Z. Mao, R. A. Scott, K. Warncke and D. G. Lynn, *Proc. Natl. Acad. Sci. U. S. A.*, 2007, **104**, 13313–13318.
26. E. D. Ciuculescu, Y. Mekmouche and P. Faller, *Chem.–Eur. J.*, 2005, **11**, 903–909.

